B.A.R.C.-1061

B.A.R.C.-1061

भारत सरकार

GOVERNMENT OF INDIA

परमाणु ऊर्जा आयोग

ATOMIC ENERGY COMMISSION

STUDY OF DEFECTS NEAR MOLYBDENUM SURFACE USING THERMAL DESORPTION SPECTROMETER

by

Pramod K. Naik
Technical Physics Division

भाभा परमाणु अनुसंधान केन्द्र

BHABHA ATOMIC RESEARCH CENTRE

बंबई, भारत

BOMBAY, INDIA

1980

B.A.R.C.- 1061

GOVERNMENT OF INDIA
ATOMIC ENERGY COMMISSION

B.A.R.C.- 1061

STUDY OF DEFECTS NEAR MOLYBDENUM SURFACE USING THERMAL DESORPTION SPECTROMETER

by

Pramod K. Naik
Technical Physics Division

BHABHA ATOMIC RESEARCH CENTRE
BOMBAY, INDIA
1980

INIS Subject Category : A 19

Descriptors :

MOLYBDENUM

POLYCRYSTALS

TARGETS

SURFACES

CRYSTAL DEFECTS

ION BEAM INJECTION

NEON IONS

ARGON IONS

KRYPTON IONS

DIFFUSION

DESORPTION

TRAPPING

ACTIVATION ENERGY

BINDING ENERGY

SPECTRA

HIGH TEMPERATURE

VERY HIGH TEMPERATURE

TEMPERATURE DEPENDENCE

ABSTRACT

Thermal desorption spectrometry is utilized to study the migration of atoms and defects near molybdenum surface. The thermal desorption spectra of inert gas ions (neon, argon and krypton) injected with various energies (430 - 1950 eV) into a polycrystalline molybdenum target with various dosages (6.4×10^{12} - 3.9×10^{14} ions/cm^2) are investigated. Four different states of binding of the trapped atoms corresponding to the activation energies for desorption have been revealed from the spectra. The activation energies are found to be relatively insensitive to the species of the bombarding ion, incident ion energy and the dosage. The patterns of the spectra are strongly influenced by the mean projected range of the ions into the solid. The activation energies deduced are in good agreement with those reported for the migration of atoms and defects in molybdenum.

STUDY OF DEFECTS NEAR MOLYBDENUM SURFACE USING THERMAL DESORPTION SPECTROMETER

by

Pramod K. Naik

1. INTRODUCTION

Recently the studies of entrapment of inert gases into solids have become increasingly important due to the fact that such entrapment and the subsequent thermal release of the trapped gas offer important clues to various phenomena related to the solid surfaces.

The work reported here involves the study of defects near polycrystalline molybdenum surface by using thermal desorption technique in ultrahigh vacuum (UHV).

Thermal desorption spectrometry(1, 2) is one of the most sensitive and powerful techniques for the study of entrapment of inert gases into solids and for the study of defect/damage in solids. It utilizes the injection of energetic ions of inert gas into the solid followed by measurement of the rate of release of gas during a specified form of temperature rise annealing process using a mass spectrometer. The temperatures at which peaks occur in the spectra correspond to the binding energies of the particular atoms trapped into the solids with different configurations. Energy, dosage and the type of the ion as well as defect/damage state of the solid near the surface influence the desorption kinetics. The precise nature of the trapping sites which gives rise to a particular peak in the spectrum can be deduced from a comparison of experimentally determined

activation energies with the calculated values of binding energies to various types of simple defect. Use of inert gas ions facilitates a straightforward collection and interpretation of experimental data.

Molybdenum is an important material associated with nuclear material technology. Blistering of molybdenum under helium ion bombardment has been studied by Erents and McCracken (3) in UHV. Migration of vacancies in molybdenum has been investigated by Suezawa and Kimura (4) by quenching experiments. Jang and Moteff (5) have studied dimensional stability of neutron-irradiated polycrystalline molybdenum using a high vacuum dilatometer, further followed by anneal study to reveal recovery stages.

Several investigations have been reported on the study of entrapment of inert gases into tungsten (6), nickel (7), uranium oxide (8), stainless steel (9) and titanium (10) using thermal desorption method. However, the entrapment of ions of heavy inert gases into molybdenum has not been investigated with this method.

In this work monoenergetic, singly charged positive ions of neon, argon and krypton of energy 430-1950 eV are injected into a clean polycrystalline molybdenum target with dosages 6.4×10^{12} - 3.9×10^{14} ions/cm^2 in UHV. Energies of different binding states of the trapped atoms are deduced from the thermal desorption spectra

taken after the injection of ions and possible mechanisms that might cause the release of gases are explained.

2. EXPERIMENTAL

Fig. 1 illustrates the symbolic diagram of the vacuum system used for the experiments. The experimental chamber is fitted with a target assembly, an ion gun, a Bayard-Alpert ionization gauge, a residual gas analyser and a metal orbitron pump. The forevacuum system consists of a sputter ion pump, two cryosorption pumps and a thermocouple gauge. A cylindrical reservoir fitted with a Barayd-Alpert ionization gauge is also connected to the experimental chamber through a UHV leak valve. The gas handling system is further connected to the reservoir through another UHV leak valve. The ultimate pressure attained in the UHV system is 1.2×10^{-10} Torr.

An ion gun designed to produce singly charged monoenergetic ions of inert gases of energy 50-2000 eV is utilized for the experiments. The electron emission current of the ion source of the gun adjustable between 0.1 - 5.0 mA is stabilized electronically. The maximum sensitivity factor of the gun for Ar^+ ions is 6.4×10^{-3} A/Torr at an electron emission current of 3×10^{-3} A.

The target is a clean, polycrystalline molybdenum sheet (1 cm x 1 cm x 0.012 cm). A Pt/Pt-Rh 13% thermocouple is utilized

to monitor the temperature of the target. For thermal desorption the target is bombarded by electrons from a filament near the target. An electron suppressor shield surrounds the target to suppress the secondary electrons during the ion bombardment. The target assembly is positioned in such a way that the ion beam can strike the central region of the target with a normal incidence.

A proportional controller is used to vary the temperature of the target from 300 K to 1573 K in 30 sec at a nearly constant rate by controlling the power to the target heating filament emitting electrons to bombard the target.

A residual gas analyzer with a 180° deflection and 1 cm radius of the ion trajectory using a 4000 Gauss permanent magnet is constructed and utilized for the measurement of the desorbed gas. It gives a 10% valley resolving power of 22 and a unit separation resolution of 30. It operates at a maximum trap current of 60 μA and can analyze ions of 2 AMU to 240 AMU.

The UHV system after the necessary processing attains an ultimate pressure of $\sim 1.2 \times 10^{-10}$ Torr.

The target is initially degassed by raising its temperature to 1600 K in UHV, before taking the measurements. Inert gas is then introduced in the experimental chamber to generate a static pressure of $\sim 1 \times 10^{-5}$ Torr with the pump isolated. At this stage the ion gun is switched on and the bombardment of the target is continued till the desired dosage is achieved. The inert gas in the experimental chamber is then pumped to attain

UHV after the dosage is complete. The temperature of the target is raised to 1573 K in 30 sec at a nearly constant rate utilizing the temperature programmer. The rate of release of gas from the target during heating is obtained as the pressure dependent ion current of the residual gas analyzer, which is differentiated and further recorded on the x-y recorder as a function of temperature to give the thermal desorption spectrum. Fig. 2 gives the schematic diagram of the thermal desorption spectrometer.

3. ACTIVATION ENERGY OF DESORPTION

The temperatures T_p at which peaks occur in the desorption spectra are determined experimentally. The values of the activation energy E_d for desorption are calculated at different values of T_p by using the relation given by Redhead (1).

$$E_d/kT_p = \ln \frac{\nu T_p}{\beta} - 3.64 \qquad \ldots (1)$$

where,

k : Boltzmann constant (8.6×10^{-5} eV/K)

ν : First order rate constant in sec^{-1}

β : The rate of rise of the temperature of the target in K/sec.

E_d and T_p are expressed in eV/atom and K respectively.

Relation (1) is derived from the relation of the rate of first order desorption from unit surface area of the solid:

$$\frac{d\sigma}{dt} = -\sigma\nu \exp(-E_d/kT) \qquad \ldots (2)$$

where σ : Number of atoms trapped per cm^2

and T : Temperature of the solid in Kelvin (K).

Relation (2) holds good for the desorption of atoms trapped within few tens of lattice constants from the surface of the solid.

Redhead (1) has given details of numerical solution for the case

$$T = T_o + \beta t \qquad \ldots\ldots (3)$$

Where T_o is the starting temperature in K of the heating cycle and β as defined in the relation (1), t being the time in sec at temperature T.

Relation (2) is solved to find the temperature T_p at which the desorption rate is maximum. Redhead has further shown that the relation between E_d and T_p is very linear, and is expressed by the relation (1) for $10^{13} > \nu/\beta > 10^8$ (K^{-1}) to $\pm$ 1.5%.

Values of E_d are determined from the desorption spectra assuming $\nu = 10^{13}$ sec^{-1} and β = 42.5 K/sec.

4. RESULTS

4.1. Variation with Dose and Energy

Fig. 3 shows the release spectra for He^+ ions incident with energy 430 eV and dosages between 2.32×10^{13} and 2.10×10^{14} ions/cm^2. Though peaks are not resolved sufficiently in neon spectra, four peaks, A, B, C and D can be seen in the spectrum taken at the dosages of 9.88×10^{13} ions/cm^2. The spectra indicate that the peak heights and the number of ions trapped increase with increasing the

dosage without causing much alteration in the general pattern of the spectra.

Fig. 4 shows the release spectra for Ar^+ ions incident with energy 430 eV and dosages between 1.18×10^{13} and 3.88×10^{14} ions/cm^2. Peaks in argon spectra are better resolved as compared to those in the case of neon. The peak heights and the numberof ions trapped for argon also increase with increasing the dosage without affecting the general pattern of the spectra.

Fig. 5 shows the release spectra for Kr^+ ions incident with energy 1225 eV and dosages between 1.01×10^{13} and 2.12×10^{14} ions/cm^2. Peaks A, B, C and D in krypton spectra are sharper than in neon and argon spectra. Krypton spectra indicate a behaviour of growth similar to that observed in the case of neon and argon.

These observations indicate that the general pattern of the spectra at a given incident ion energy is not affected by the variation of the ion dosage which causes only a corresponding variation in the peak heights thus indicating that the number of ions trapped is proportional to the number of ions incident at a given energy. This observation agrees with the studies with tungsten (6) and nickel (7) by earlier workers.

Fig. 6 shows neon release spectra taken at a common dosage $\sim 1.2 \times 10^{14}$ ions/cm^2 for different incident energies between 430 and 1950 eV. Similar sets of spectra for argon and krypton are shown in Figs. 7 and 8 respectively. It can be observed that in each case the change in general pattern of the spectra due to the predominance of peak D has occured at incident ion energies just below 740, 975 and

1470 eV for neon, argon and krypton respectively and that the pattern does not exhibit much change at higher incident energies.

4.2 Influence of the Projected Range of Ions

Fig. 9 shows the release spectra of Ne^+ ions of 430 and 740 eV, Ar^+ ions of 740 and 975 eV and Kr^+ ions of 1225 and 1470 eV, all taken with a common ion dosage of 1.2×10^{14} ions/cm^2. These spectra are selected to indicate transition in their pattern with increase in the incident ion energy due to predominance of peak D. Calculations based on Schiott's model (11) indicate that the approximate projected range of the respective ions during such transitions is 10 Å.

Thus it can be confirmed that the pattern of the release spectra, defined by the relative heights of the peaks is characteristic of the depth of ion penetration.

4.3 Energies:

In view of lack of adequate resolution, an accurate deconvolution of spectra is not possible and no attempt has been made to quantify the individual peak populations and the trapping probabilities.

It is clear from the spectra observed that all the release transients are considerably broader than those expected due to first order desorption from sites of a single discrete activation energy. Individual values of the binding energy calculated from the positions of the peaks are therefore treated as being representative and correspond to the most probable activation energies

about which it is recognised that there is a spread.

Activation energies for desorption corresponding to the peaks A, B, C and D in the spectra are calculated as described in Section 3 earlier and their values are given in Table 1.

Table - 1

Activation Energies of Desorption for Neon, Argon and Krypton in Molybdenum

	A Energy (eV)	B Energy (eV)	C Energy (eV)	D Energy (eV)
Neon	1.05 - 1.27	1.92	2.54 - 2.94	3.50 - 3.75
Argon	1.05 - 1.50	1.92 - 2.17	2.60 - 2.74	3.39 - 3.61
Krypton	0.94 - 1.23	2.04 - 2.22	2.59 - 2.65	3.21 - 3.53

4.4 Possible Mechanisms for Release

The nature of the trapping site which gives rise to a particular peak in the desorption spectra can be deduced from the comparison of the values of activation energies determined experimentally with those associated with the motion of atoms and defects in the solid.

4.4.1 State A

State A of the binding energy with values 0.94 - 1.50 eV is associated with a temperature range of 385 - 595 K. The peaks observed in this state are particularly prominent for krypton at all

incident ion energies utilized while they can be seen clearly in case of argon and neon at lower incident ion energies only. The peaks are characteristic of the possible entrapment at sites immediately below the surface. It is possible that the release in this state is effected by the diffusion of the impurities at the surface and at grain boundaries.

Yoshioka and Kimura (12) in their studies on precipitation of carbon impurities in polycrystalline molybdenum using resistivity measurements, have suggested that carbon atoms may migrate with an activation energy smaller than 1.5 eV. Niebel and Wilkens (13) have interpreted the results of their previous work (14) on the analysis of the neutron-irradiated molybdenum in terms of nucleation and growth of interstitial loops using a theory of Brown et al (15). They have estimated a value of 0.9 eV for the binding energy of the interstitial to the impurity atom. They further suggested that different species of impurities might have different binding energies. The values of the binding energy of State A are close to those reported above.

4.4.2 State B

Values of binding energy between 1.92 and 2.22 eV corresponding to a temperature range of 755 - 875 K have been associated with State B. State B is believed to be related to vacancy motion at the surface, allowing release of the trapped atoms situated below the surface. The values of the binding energy observed for this state are close to the value of 2.2 eV for the energy of vacancy migration in molybdenum

reported by Nihoul (16) and Flynn (17). In their theoretical work using a method of direct minimization of the potential energy of the real space atomic configuration, Kenny and Heald (18) have calculated a value of 2.3 eV for vacancy migration in molybdenum. The experimental values for this state are also close to the value 1.9 eV for the energy for defect migration in molybdenum reported by Mamaluy et al (19).

4.4.3 State C

State C of the binding energy with values 2.54 - 2.94 eV corresponds to a temperature range of 1000 - 1150 K. This state is attributed to the release of trapped atoms effected by the self-diffusion of the host atoms at the surface. The value 2.46 eV reported by Bettler et al (20) for the activation energy of self-diffusion on the surface of clean molybdenum using field emission patterns is close to the values obtained in the State C. Singer (21) studied the self-diffusion on ultra-clean molybdenum single crystal surfaces using the sinusoidal surface grooves decay technique in UHV. The values of activation energy for self-diffusion at the surface reported by him were different for different crystallographic planes. The value 2.99 eV reported by him for (110) molybdenum surface is close to the values experimentally determined for the activation energy of desorption for State C. Using similar techniques, Allen (22) reported a value of 2.43 eV for the activation energy for surface self-diffusion of molybdenum.

4.4.4 State D

As discussed earlier in Section 4.1, the spectra selected in Fig. 4 indicate transition in their pattern with increase in the incident ion energy due to predominance of peak D. It has been established that the transition is associated with an approximate projected range of 10 Å of the respective ions in molybdenum.

Values of binding energy between 3.21 and 3.75 eV, corresponding to a temperature range of 1255 - 1475 K have been associated with the State D. This state appears to be connected with the desorption of trapped atoms effected by motion in the region 3-4 atomic layers or further deep into molybdenum. Askill and Tomlin (23) used the radioactive isotope molybdenum-99 to study self-diffusion in polycrystalline and single crystal specimens of molybdenum. The values of activation energy for self-diffusion in molybdenum reported by them are 3.99 eV and 4.2 eV for single crystal and polycrystalline specimens respectively. Similar techniques utilized by Pavlinov and Bykov (24) reported a value of 4.77 eV for a polycrystalline sample. Zakurdaev (25) used inert marker movement to study electro and thermo-transport in molybdenum single crystals. Information on the diffusion near the surface was deduced from the development of a step-like surface structure. The activation energy for self-diffusion determined from the experiments is 4.4 eV. Kalinovich et al (26) have recently reported 4.59 eV as the value for the activation energy for bulk self-diffusion in molybdenum by using

a radiotracer technique.

Values of binding energy in this state are believed to be associated with the self-diffusion of the host atoms in the region of entrapment, effecting the release of the trapped atoms. From an estimate of the threshold temperatures of the peaks in the State D, activation energy in the range 3.21 - 3.50 eV can be calculated. These values are considerably lower than those available for the self-diffusion of the host atoms in the bulk (3.99 - 4.77 eV). This may be attributed to the fact that the majority of trapping sites for this state are situated in a region 3 to 4 atomic layers deep from the surface. The values of the activation energy of migration of the host atoms characteristic of this region with its proximity to the surface are expected to lie inbetween those at the surface and in the bulk.

4.5 CONCLUSIONS

The activation energies of desorption are found to be relatively insensitive to the species of the bombarding ion, incident ion energy and the dosage used. A strong influence of the mean projected range of the ions penetrating into the solid on the general pattern of the spectra has been revealed in the experiments. Four different states A, B, C and D of binding exhibited by the spectra appear to have been influenced by the proximity of the surface from the trapping sites. State A is thought to arise from the diffusion of impurities at the surface and at grain boundaries. State B (1.92 - 2.22 eV) is believed to be related to vacancy motion at the

surface. State C (2.54 - 2.94 eV) is attributed to the release of atoms effected by the self-diffusion of the host atoms on the surface. State D appears to be connected with the migration of molybdenum atoms in the region 3-4 atomic layers or further deep into the solid. It is clear from the results that the injection of energetic ions of inert gas into the solid followed by the thermal desorption in UHV can offer important clues to migration processes occuring near the solid surface.

ACKNOWLEDGEMENTS:

I am thankful to V.G. Kagal, S.L. Verma and S.P. Bhaskar for the instrumentation essential for the work. I am indebted to A.S. Divatia for many fruitful discussions. I wish to thank R.Y. Deshpande for encouragement during the work.

REFERENCES

1. P.A. Redhead, Vacuum 12, 203 (1962).

2. G. Carter, Vacuum, 12, 245 (1962).

3. S.K. Erents and G.M. McCracken, Radiation Effects, 18, 191 (1973).

4. M. Suezawa and H. Kimura, Proc. Conf. on Defect Clusters in BCC Metals and their Alloy, NBS, Gaithersburg, Md. U.S.A. p.440 (1973).

5. H.I. Jang and J. Motefi ASTM,STP 570, p. 404 (1975).

6. E.V. Kornelsen, J. Vac. Sci. Technol. 6, 173 (1969).

7. D. Edwards Jr., J. Appl. Phys. 46, 1437 (1975).

8. A.P.R. Cavaleru and F. Vasiliu, Rev. Roum. Phys. 19, 287 (1974).

9. D.J. Reed, F.T. Harris, D.G. Armour and G. Carter, Vacuum, 24 179 (1974).

10. T.D. Radzhabov and G.F. Ivanovskii, Sov. Phys. - Tech. Phys. 11, 1539 (1967).

11. H.E. Schiott, Radiation Effects, 6, 107 (1970).

12. K. Yoshioka and Y. Kimura, Ind. J. Technol, 11 547 (1973).

13. K. Niebel and M. Wilkens, Phys. Stat. Sol. (a) 25, 77 (1974).

14. K. Niebel and M. Wilkens, Phys. Stat. Sol. (a) 24, 591 (1974).

15. L.M. Brown, A. Kelly and A.M. Meyer, Phil. Mag. 19, 721 (1969).

16. J. Nihoul, "Vacancies and Interstitials in Metals", Ed.A. Seeger, D. Schumacher, W. Schilling and J. Diehl, North Holland, Amsterdam p. 839 (1970).

17. C.P. Flynn, Phys. Rev. 179, 920 (1969).

18. P.W. Kenny and P.T. Heald, Phil. Mag. 29, 1137 (1974).

19. A.A. Mamaluy, V.A. Pervakov and V.I. Khotkevich, Fiz. Metal, Metalloved, 36 , 1101 (1973).

20. P.C. Bettler, D.H. Bennum and C.M. Case, Surface Sci. 44, 360 (1974).

21. K.E. Singer, Colloq. Intl. Cent. Nat. Rech. Sci. No. 187, p. 199 (1970).

22. B.C. Allen, Metallurgical Trans. 3 , 2344 (1972).

23. J. Askill and D.H. Tomlin, Phil. Mag. 8, 997 (1963).

24. L.V. Pavlinov and V.N. Bykov, Fiz. Metal Metalloved, 18, 459 (1964).

25. I.V. Zakurdaev, Fiz. Tverd. Tela, 11, 3463 (1963).

26. D.F. Kalinovich, I.I. Kovenskii and M.D. Smolin, Izv. Vyssh. Uchebn. Zaved Fiz. 20, 148 (1977).

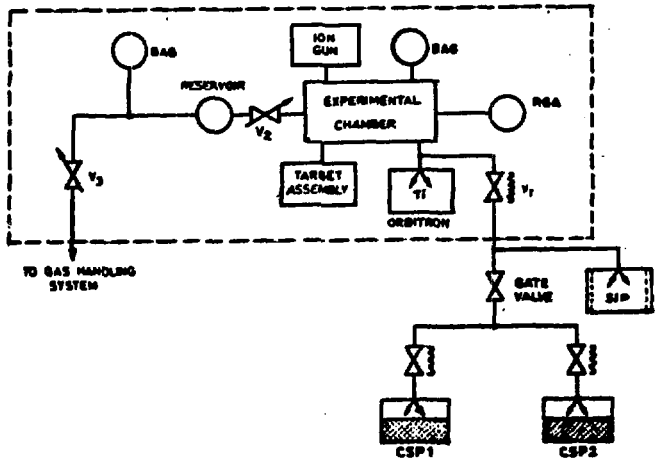

FIG. 1 SYMBOLIC DIAGRAM OF THE VACUUM SYSTEM

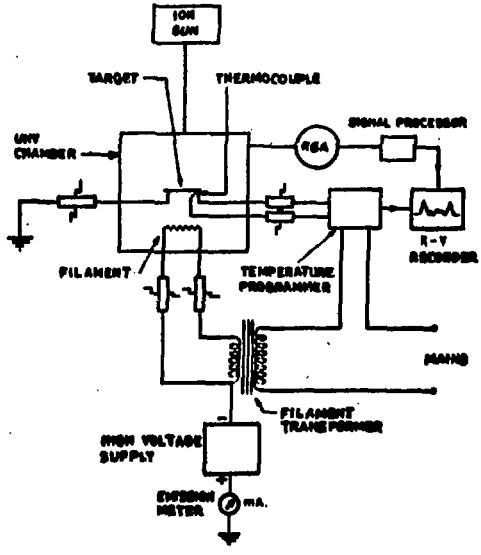

FIG. 2 SCHEMATIC DIAGRAM OF THE THERMAL DESORPTION SPECTROMETER

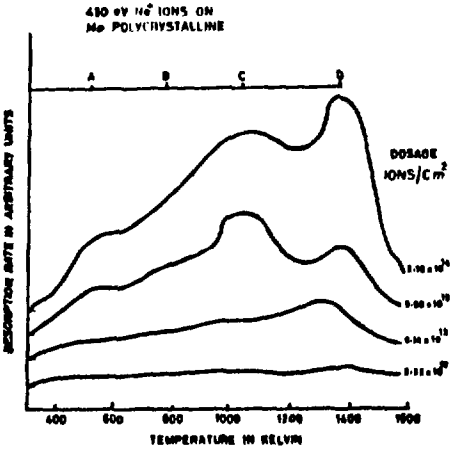

FIG. 3 DESORPTION SPECTRA FOR 430 eV Ne^+ IONS

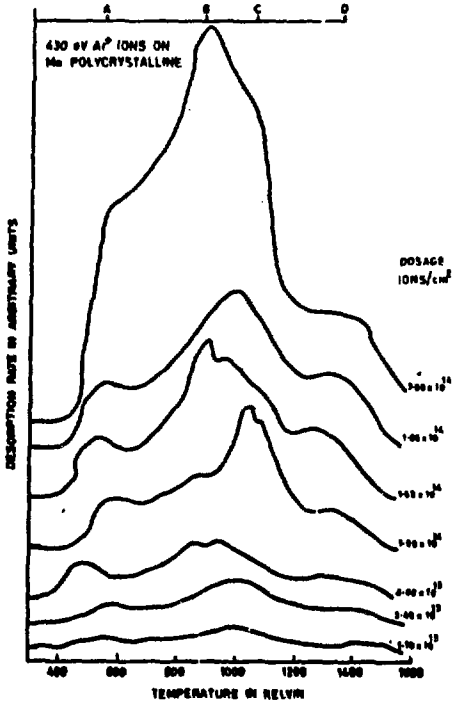

FIG. 4 DESORPTION SPECTRA FOR 430eV Ar^+ IONS

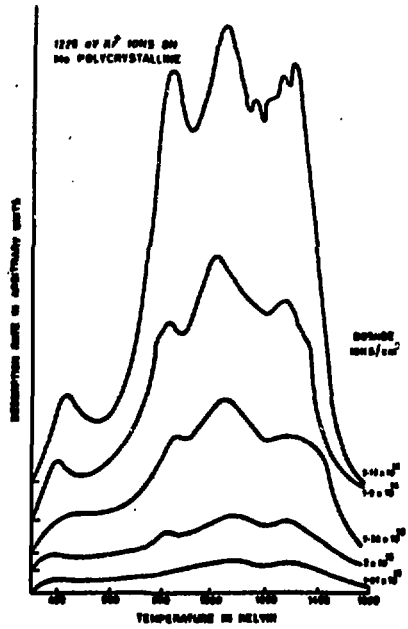

FIG. 5 DESORPTION SPECTRA FOR 1225 eV $Kr^{\oplus}$ IONS

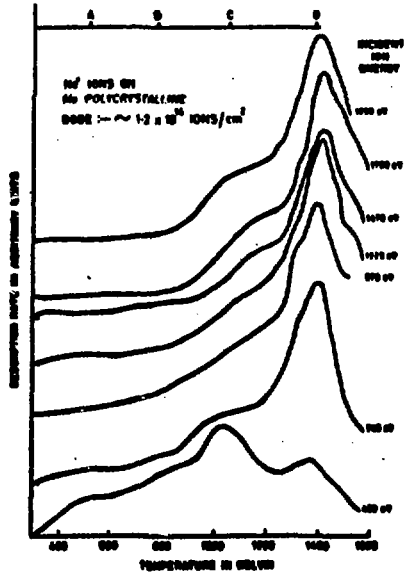

FIG. 6 DESORPTION SPECTRA FOR $Ne^{\oplus}$ IONS WITH A DOSE ~1·2 X 10^{14} IONS/cm^2

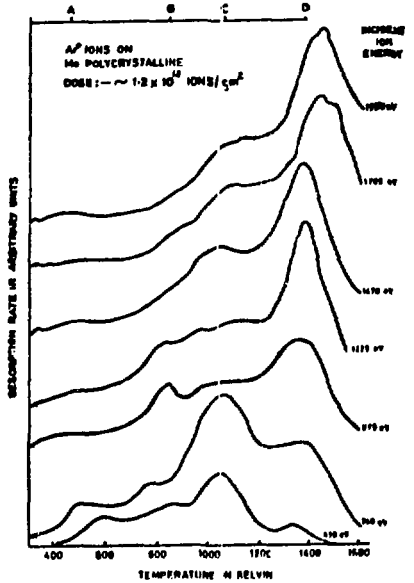

FIG. 7 DESORPTION SPECTRA FOR Ar^+ IONS WITH A DOSE ~1·2 X 10^{14} IONS/cm^2

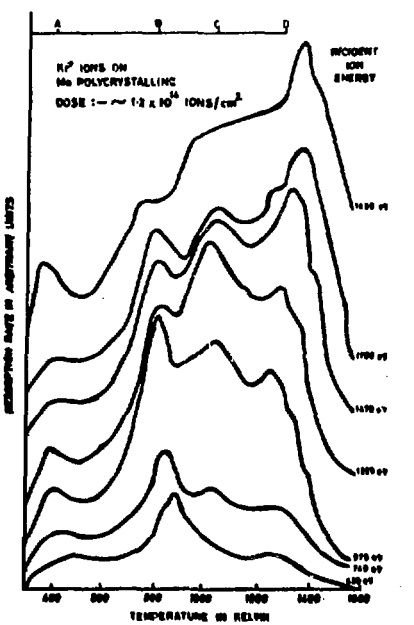

FIG. 8 DESORPTION SPECTRA FOR Kr^+ IONS WITH A DOSE ~ 1·2 X 10^{14} IONS/cm^2

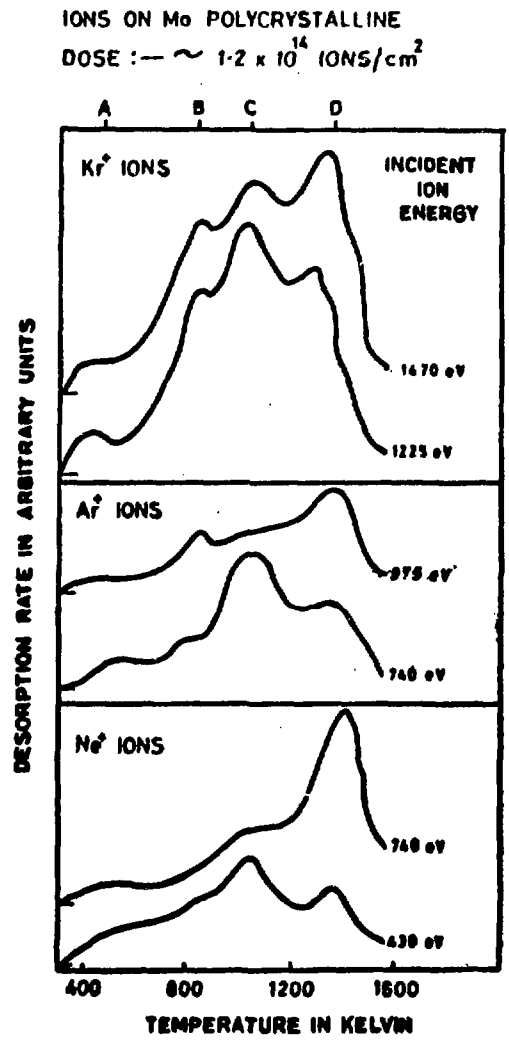

FIG. 9 DESORPTION SPECTRA FOR Ne^+, Ar^+ AND Kr^+ IONS INDICATING TRANSITION IN PATTERN